

Observational Consequences of GRBs as Sources of Ultra High Energy Cosmic Rays

Soebur Razzaque^{*,†}, Charles D. Dermer^{*}, Justin D. Finke^{*,†} and Armen Atoyan^{**}

^{*}*Space Science Division, U.S. Naval Research Laboratory, Washington, DC 20375, USA*

[†]*National Research Council Research Associate*

^{**}*Concordia University, Montreal, Quebec H3G 1M8, Canada*

Abstract. Gamma-ray bursts (GRBs) have long been considered as candidates of ultrahigh-energy cosmic rays (UHECRs). We investigate the signatures of CR proton acceleration in the GRBs by consistently taking into account their hadronic and electromagnetic interactions. We discuss the implications of our findings for high-energy gamma ray observations with the recently launched *Fermi Gamma-ray Space Telescope*.

Keywords: gamma rays: bursts—gamma rays: theory—radiation mechanisms: nonthermal

PACS: 98.70.Sa, 98.70.Rz

INTRODUCTION

Gamma-ray bursts are the most powerful explosions in the universe releasing about 10^{51} ergs of energy in keV–MeV γ -rays within tens of seconds. Emission of this non-thermal radiation via synchrotron and/or Compton scattering requires acceleration of electrons to very high energies, probably by a Fermi mechanism in relativistic shocks. Rapid variability time scales ($t_v \sim 0.001$ – 1 s) observed in non-thermal γ -ray light curves implies that the emission region is compact and moves with a large bulk Lorentz factor ($\Gamma \sim 100$ – 1000) towards the observer.

In the context of the fireball shock model (see, e.g., Refs. [1, 2] for reviews), successively ejected materials in the form of fireballs from a central engine (black hole or a magnetar) collide with each other, due to differences in their bulk Lorentz factors, forming relativistic forward and reverse shocks (internal shocks). A baryonic (assumed mostly protons) contamination/load in an otherwise pure e^\pm and γ dominated fireball or the energy release from the central engine may change in time and lead to a varying bulk Lorentz factor. Thus a baryonic component is required in this model to explain rapid γ -ray variability.

Protons can be accelerated to UHE in the same shock which may be responsible for electron acceleration in the GRB jet [3]. The energy losses and size scale of the shocked region limit, however, the maximum proton energy. Synchrotron radiation and photohadronic ($p\gamma$) interactions are dominant energy loss channels for the UHE protons and the lost energy is converted to high-energy γ -rays and neutrinos [4, 5, 6, 7, 8, 9, 10, 11]. The acceleration of protons to UHE takes place on a longer time scale than the acceleration of electrons in the shocks. Therefore, a characteristic time delay is expected for proton-induced high-energy γ -ray and neutrino emission as compared to the keV–MeV emission by electrons via synchro-Compton mechanism(s). We discuss these signatures of UHE cosmic ray acceleration in the GRB jet as currently being probed by the Large Area Telescope (LAT) and the Gamma-ray Burst Monitor (GBM) onboard the *Fermi Gamma-ray Space Telescope*.

PROTON ACCELERATION AND ENERGY LOSSES

The γ -ray spectrum in the keV–MeV range is well-fitted by the Band function [12] which is defined as

$$\mathcal{B}(\varepsilon) = \mathcal{A} \times \begin{cases} (\varepsilon/100 \text{ keV})^\alpha \exp(-\varepsilon/\varepsilon_0) ; \varepsilon < (\alpha - \beta)\varepsilon_0 \\ [(\alpha - \beta)(\varepsilon_0/100 \text{ keV})]^{\alpha - \beta} \exp(\beta - \alpha)(\varepsilon/100 \text{ keV})^\beta ; \varepsilon \geq (\alpha - \beta)\varepsilon_0 , \end{cases} \quad (1)$$

where ε is the photon energy measured in keV and \mathcal{A} is the normalization factor measured in units of photons $\text{cm}^{-2} \text{s}^{-1} \text{keV}^{-1}$ at 100 keV. An integration of the quantity $\varepsilon \mathcal{B}(\varepsilon)$ over a given energy band (which we assumed to be 1 keV – 1 GeV throughout our calculation) and time interval gives the fluence \mathcal{S} (e.g., in units of ergs cm^{-2})

TABLE 1. Derived quantities from Band function parameters: $\alpha = -1$, $\beta = -2.2$, $\varepsilon_0 = 10^3$ keV, $\mathcal{A} = 10^{-2}$ ph cm $^{-2}$ keV $^{-1}$ at 100 keV, and $z = 2$ for a 10 s long GRB

t_v (s)	\mathcal{S} (ergs cm $^{-2}$)	\mathcal{E} (ergs)	Γ	$R = \Gamma R'$ (cm)	$B' \sqrt{\varepsilon_B/\varepsilon_e}$ (G)
10^0	3.2×10^{-5}	3.2×10^{53}	385	1.5×10^{15}	6.3×10^3
10^{-1}	–	–	550	3.0×10^{14}	2.2×10^4
10^{-2}	–	–	790	6.2×10^{13}	7.3×10^4
10^{-3}	–	–	1135	1.3×10^{13}	2.5×10^5

in that energy and time range. The total isotropic-equivalent energy release from a burst at redshift z and luminosity distance d_L is $\mathcal{E} = 4\pi d_L^2 \mathcal{S} / (1+z)$.

The proper number density of photons (e.g., in units of photons cm $^{-3}$ keV $^{-1}$) in the comoving fireball frame (all variables are primed in this frame) can be obtained from the Band function as

$$n'_\gamma(\varepsilon') \simeq \frac{2d_L^2}{\Gamma^4 t_v^2 c^3} \mathcal{B} \left(\frac{\varepsilon' \Gamma}{1+z} \right), \quad (2)$$

where $\varepsilon' = \varepsilon(1+z)/\Gamma$ and the size of the emitting region is $R' \approx \Gamma t_v c / (1+z)$. The energy density of photons in the comoving frame is $U'_\gamma = \int_{\varepsilon'_{\min}}^{\varepsilon'_{\max}} \varepsilon' n'_\gamma(\varepsilon') d\varepsilon'$. The energy density of baryons is assumed to be $U'_p = U'_\gamma / \varepsilon_e$, where $\varepsilon_e < 1$, in the fast-cooling scenario. The magnetic energy density is $U'_B = B'^2 / 8\pi = \varepsilon_B U'_p$, and the magnetic field is $B' = \sqrt{8\pi(\varepsilon_B/\varepsilon_e)U'_\gamma}$ with $\varepsilon_B < 1$. We choose the typical Band function parameters $\alpha = -1$, $\beta = -2.2$, $\varepsilon_0 = 1$ MeV, $\mathcal{A} = 10^{-2}$ ph cm $^{-2}$ keV $^{-1}$ and $z = 2$ (corresponding to $d_L \simeq 4.85 \times 10^{28}$ cm for the standard Λ CDM cosmology), and we have listed in Table 1 different derived quantities for $t_v = 10^{-3}$ –1 s and for 1 keV $\leq \varepsilon \leq 1$ GeV. We assumed that Γ is the same as Γ_{\min} which has been derived using the condition that the fireball becomes optically thin to $\gamma\gamma \rightarrow e^\pm$ pair production at 1 GeV (see, e.g., Refs. [13, 7, 14]).

The acceleration time scale for protons in the electric field induced by B' is proportional to the Larmor time (E'_p/eB') and is given by

$$t'_{p,\text{acc}} = \frac{\phi \hbar}{m_p^2 c^4} \frac{B_{\text{cr}}}{B'} E'_p \simeq 11 \frac{\phi E'_{p,9}}{B'_4} \text{ s}, \quad (3)$$

where $B_{\text{cr}} = m_p^2 c^3 / e \hbar = 1.488 \times 10^{20}$ G, $B' = 10^4 B'_4$ G, $E'_p = 10^9 E'_{p,9}$ GeV and $\phi \gtrsim 1$ is the number of gyro-radii required to increase a particle energy by a factor of 2.7. The synchrotron cooling time for protons in the same magnetic field is

$$t'_{p,\text{syn}} = \frac{9}{4} \frac{\hbar^2}{r_e m_e c} \frac{B_{\text{cr}}^2}{B'^2} \frac{1}{E'_p} \simeq \frac{45}{B'_4{}^2 E'_{p,9}} \text{ s}. \quad (4)$$

The photohadronic cooling time scale, which does not depend on the magnetic field but on the observed keV–MeV γ -ray source density in equation (2), is given by

$$t'_{p\gamma}{}^{-1} = \frac{m_p^2 c^5}{2E_p'^2} \int_0^\infty d\varepsilon' \frac{n'_\gamma(\varepsilon')}{\varepsilon'^2} \int_0^{2E_p'\varepsilon'/m_p c^2} d\varepsilon'_r \sigma_{p\gamma}(\varepsilon'_r) f(\varepsilon'_r) \varepsilon'_r \simeq c \sigma_0 \int_{\varepsilon'_{\text{th}} m_p c^2 / 2E_p'}^\infty d\varepsilon' n'_\gamma(\varepsilon') \quad (5)$$

for single $p\gamma$ scattering. We approximated a $p\gamma$ cross-section of $\sigma_0 \equiv \sigma_{p\gamma}(\varepsilon'_r) f(\varepsilon'_r) = 68 \mu\text{b}$ for $\varepsilon'_r \geq \varepsilon'_{\text{th}}$ following Ref. [15]. Here $\varepsilon'_r = \varepsilon'(1 - \beta_p \cos \theta) E_p' / m_p c^2$ is the photon energy evaluated in the proton's rest frame for the angle θ between the directions of the proton and target photon, and we take $\varepsilon'_{\text{th}} \simeq 0.2$ GeV as the threshold photon energy for pion production in the rest frame of the proton.

We have plotted in Fig. 1 different time scales for protons with the assumed Band function parameters, redshift and four different variability time scales (see Table 1). Two sets of three straight lines, with positive and negative slopes, correspond to acceleration and synchrotron cooling times respectively, for $\varepsilon_B/\varepsilon_e = 10$ (dashed lines), 1 (solid lines) and 0.1 (dot-dashed lines) in Table 1. The horizontal solid line in each panel correspond to the dynamic time $t'_{\text{dyn}} \approx t_v \Gamma / (1+z)$. The vertical thick-dashed line is the proton escape time $t'_{\text{esc}} = (3/2)(m_p^2 c^4 / \hbar)(B'/B_{\text{cr}}) t_{\text{dyn}}^2 / E_p'$ in the Bohm diffusion limit, plotted for the proton energy at which $t'_{\text{esc}} = t'_{\text{dyn}}$. Note that for all four t_v plotted in Fig. 1, synchrotron cooling effectively determines the maximum proton energy if $\varepsilon_B/\varepsilon_e \gtrsim 1$. The photohadronic cooling

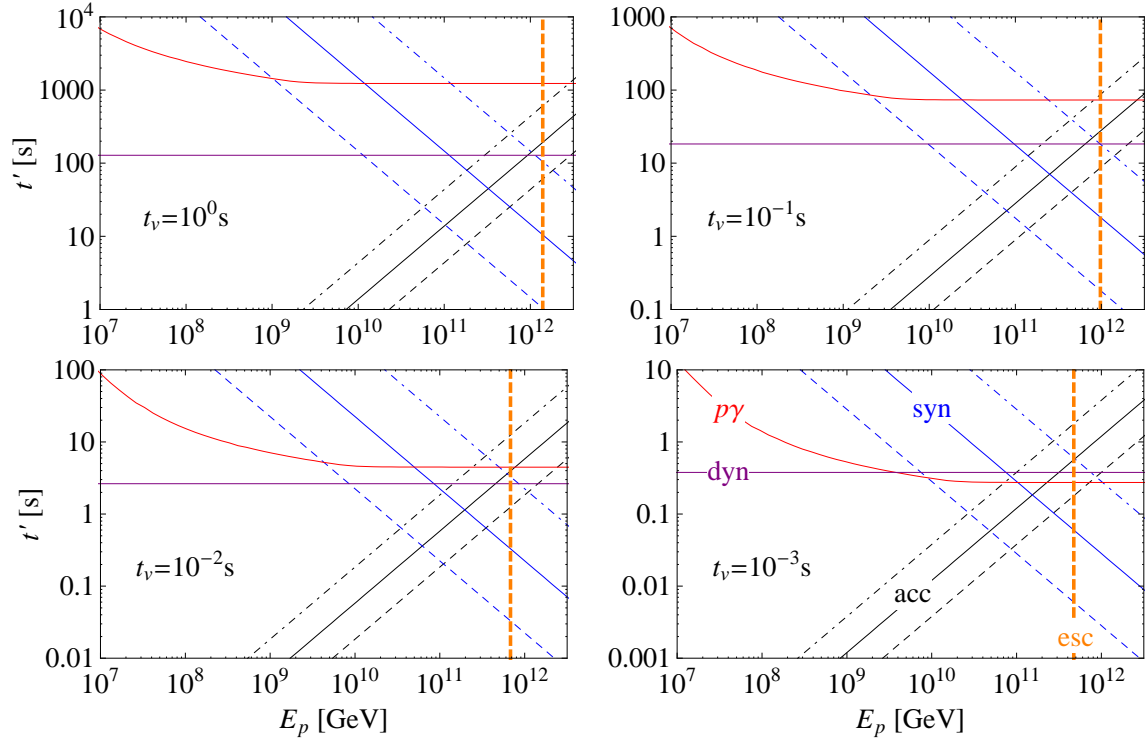


FIGURE 1. The acceleration and cooling times (labeled in the lower-right panel) for protons for the GRB parameters assumed in Table 1 with different t_v . The dashed, solid and dot-dashed curves in the sets labeled “acc” and “syn” are for $\epsilon_B/\epsilon_e = 0.1, 1$ and 10 respectively. We used the Band function in equation (1) in the $1 \text{ keV} - 1 \text{ GeV}$ observed photon energy range with derived parameters given in Table 1, and $\phi = 1$ in equation (3) for our calculation. The maximum proton energy can be read off from a plot when the “acc” curve, for a given B' field, is intersected by one of the cooling curves “ $p\gamma$ ” or “syn” for the same B' field, or by the “dyn” curve. The top left panel for $t_v = 1 \text{ s}$ and $\epsilon_B/\epsilon_e = 1$ correspond to $E_{p,\text{max}} \simeq 3 \times 10^{20} \text{ eV}$, the highest among all choices of the parameters t_v and ϵ_B/ϵ_e . See main text for details.

(smoothly-curved solid line labeled $p\gamma$) is important for highly variable GRBs as the internal photon density [see equation (2)] increases to allow frequent interactions by high-energy protons. The protons may not escape the shocked region for the parameters assumed here.

Proton-synchrotron radiation and photohadronic interactions (via π^0 decays) produce very high-energy photons. Photohadronic interactions also produce very high-energy electrons (via π^+ decays). These particles initiate electromagnetic cascades in the GRB fireball. We postpone the details of the cascade modeling and emission for future work. In the next section we concentrate on an analytic estimate of the proton-synchrotron radiation, which dominates for $\epsilon_B/\epsilon_e \gtrsim 1$ in the GRB fireball. Note that, in this limit the Compton parameter $Y = (-1 + \sqrt{1 + 4\epsilon_e/\epsilon_B})/2 \lesssim 1$ in the fast-cooling scenario and the Compton scattering of synchrotron photons to high-energy γ -rays (SSC) may not be important [16].

PROTON SYNCHROTRON RADIATION

Assuming that synchrotron radiation limits proton acceleration, the maximum shock-accelerated proton energy as a function of time in the shocked fluid frame is

$$E'_{p,\text{max}}(t') = \begin{cases} \frac{m_p^2 c^4}{\phi \hbar} \frac{B'}{B_{\text{cr}}} t' ; & 0 \leq t' < t'_{p,0} \\ \left(\frac{9 \hbar m_p^2 c^3}{4 \phi r_{\text{em}e}} \frac{B_{\text{cr}}}{B'} \right)^{1/2} ; & t'_{\text{dyn}} \geq t' \geq t'_{p,0} \end{cases} \quad (6)$$

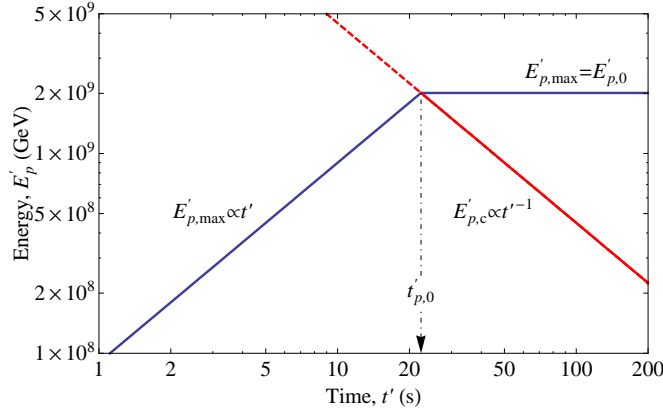


FIGURE 2. Maximum shock-accelerated energy ($E'_{p,max}$) and characteristic synchrotron cooling energy ($E'_{p,c}$) for protons as functions of the comoving time. Note that the synchrotron cooling is important for $t' \geq t'_{p,0}$ where $t'_{p,0}$ is denoted by the arrow.

The maximum proton energy in the second case in equation (6) is found from the condition $t'_{p,acc} = t'_{p,syn}$ and the time to accelerate protons to this maximum energy are given by

$$E'_{p,0} = \left(\frac{9 \hbar m_p^2 c^3 B_{cr}}{4 \phi r_e m_e B'} \right)^{1/2} \approx \frac{2 \times 10^9}{\phi^{1/2} B_4^{1/2}} \text{ GeV, and} \quad (7)$$

$$t'_{p,0} = \left(\frac{9 \phi \hbar^3 B_{cr}^3}{4 r_e m_e m_p^2 c^5 B'^3} \right)^{1/2} \approx 22 \frac{\phi^{1/2}}{B_4^{3/2}} \text{ s,} \quad (8)$$

respectively. Thus for $t' \geq t'_{p,0}$ the maximum proton energy remains constant at $E'_{p,0}$ (see Fig. 2). The synchrotron cooling, however, becomes significant with increasing time. The characteristic synchrotron cooling-break energy for protons from the condition $t'_{p,syn} = t'$, and for $t'_{dyn} \geq t' \geq t'_{p,0}$ is given by (see Fig. 2)

$$E'_{p,c}(t') = \frac{9 \hbar^2 B_{cr}^2}{4 r_e m_e c B'^2} \frac{1}{t'} \approx \frac{5 \times 10^8}{B_4^2 t_2'} \text{ GeV,} \quad (9)$$

where $t_2' = t'/100$ s. Protons above this energy cool efficiently down to $E'_{p,c}(t')$ within t' . As a result the proton spectrum can be approximated by a broken power law with the spectral index softened by unity for $E'_p > E'_{p,c}$ [17].

The number density of particles behind the shock is $4n'\Gamma_{rel}$, where n' is the pre-shock number density in the GRB fireball. As the shock crosses the fireball, it sweeps-up particles and the number density of shocked particles increases $\propto t'$. We assume that a time-dependent fraction of the shock energy density $4n'm_p c^2 \Gamma_{rel}^2$ is channeled to the high energy protons. In the most optimistic scenario, the time-dependent proton number spectrum can be written as

$$n'_p(E'_p, t') \approx 4n' \frac{t'}{t'_{dyn}} C_p \times \begin{cases} (E'_p/E'_{p,min})^{-\kappa}; & E'_{p,min} \leq E'_p < E'_{p,c}(t') \\ (E'_{p,c}/E'_{p,min})(E'_p/E'_{p,min})^{-\kappa-1}; & E'_{p,c}(t') \leq E'_p \leq E'_{p,max}(t') \end{cases} \quad (10)$$

where C_p is an overall normalization factor and $E'_{p,min} \sim \Gamma_{rel} m_p c^2$ is the minimum proton energy, and $\Gamma_{rel} \sim 1-10$ is the relative Lorentz factors between two colliding shells. The snapshot of this spectrum is plotted in Fig. 3 at different t' , and for arbitrarily fixed n' and C_p .

The synchrotron power and the typical synchrotron photon energy emitted by a proton of energy E'_p are given by

$$P'(E'_p) = \frac{4 r_e m_e c B'^2}{9 \hbar^2 B_{cr}^2} E_p'^2, \text{ and} \quad (11)$$

$$\epsilon'_o = \frac{3 B'}{2 B_{cr}} \frac{E_p'^2}{m_p c^2}, \quad (12)$$

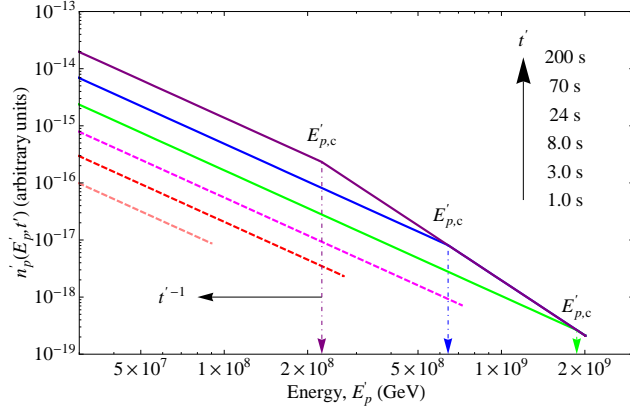


FIGURE 3. Shock-accelerated proton spectrum at increasing comoving time (from bottom to top). Total number of protons swept-up by the shock increases linearly with time as in equation (10). At early times, $t' < t'_{p,0}$ in equations (6) and (8), the maximum proton energy increases linearly (dashed lines) and saturates to a constant value $E'_{p,0}$ given in equation (7) for $t' \geq t'_{p,0}$ (solid lines). As the synchrotron cooling becomes important for $t' \geq t'_{p,0}$, the spectrum shows a break at $E'_{p,c}$ given in equation (9) which decreases with time as $\propto t'^{-1}$. The spectrum is $\propto E'^{-\kappa}$ below $E'_{p,c}$ and $\propto E'^{-\kappa-1}$ above $E'_{p,c}$.

respectively. For the characteristic proton synchrotron cooling energy in equation (9), the typical synchrotron photon energy from equation (12) for $t'_{\text{dyn}} \geq t' \geq t'_{p,0}$ is

$$\epsilon'_{o,c}(t') = \frac{243}{32} \frac{\hbar^4 B_{\text{cr}}^3}{r_e^2 m_e^2 m_p c^4 B^3} \frac{1}{t'^2} \approx \frac{22}{B_4^3 t_2^2} \text{ GeV}. \quad (13)$$

The ratio of the synchrotron power to the typical photon energy roughly gives the spectral power. The total spectral emissivity (e.g., in units of $\text{ergs cm}^{-3} \text{ s}^{-1} \text{ GeV}^{-1}$) from all protons with energy $E'_{p,c}$ from the distribution in equation (10) is given by

$$\mathcal{P}'_{\epsilon'_{o,c}}(t') \approx \frac{P'(E'_{p,c}(t'))}{\epsilon'_{o,c}(t')} \times n'_p(E'_{p,c}, t') \approx \frac{8}{27} \frac{r_e m_e m_p c^3 B'}{\hbar^2 B_{\text{cr}}} n'_p(E'_{p,c}, t'). \quad (14)$$

The corresponding time-dependent energy flux (e.g., in units of $\text{ergs cm}^{-2} \text{ s}^{-1}$) of the proton synchrotron radiation, in analogy with electron synchrotron radiation in the slow-cooling regime [17], is

$$\mathcal{F}'_{\epsilon'}(t') \propto E'_{p,c} \mathcal{P}'_{\epsilon'_{o,c}}(t') \times \begin{cases} (\epsilon'/\epsilon'_{\min})^{1/3}; & \epsilon' < \epsilon'_{\min} \\ (\epsilon'/\epsilon'_{\min})^{-(\kappa-1)/2}; & \epsilon'_{\min} \leq \epsilon' \leq \epsilon'_{o,c}(t') \\ (\epsilon'_{o,c}/\epsilon'_{\min})^{-(\kappa-1)/2} (\epsilon'/\epsilon'_{o,c})^{-\kappa/2}; & \epsilon'_{o,c}(t') \leq \epsilon' \leq \epsilon'_{\max}(t'). \end{cases} \quad (15)$$

Here ϵ'_{\min} and ϵ'_{\max} are respectively the typical photon energies for the protons with energies $E'_{p,\min}$ and $E'_{p,\max}$. We have plotted this proton synchrotron radiation spectrum at different times $t' \geq t'_{p,0}$ in Fig. 4. High energy photons $\epsilon' \gtrsim \text{MeV}$, however, produce e^\pm pairs which initiate cascades. Note that the proton synchrotron radiation and the cascade radiation build-up gradually with time as the shock propagates through the GRB fireball. As a result, high-energy emission from proton synchrotron radiation would be delayed compared to the prompt keV–MeV emission from shock-accelerated primary electrons.

DISCUSSION

We have investigated different scenarios of fireball shock model for GRBs in which protons can be accelerated to ultrahigh energies and produce observable γ -ray signatures. We found that — for the Band function parameters

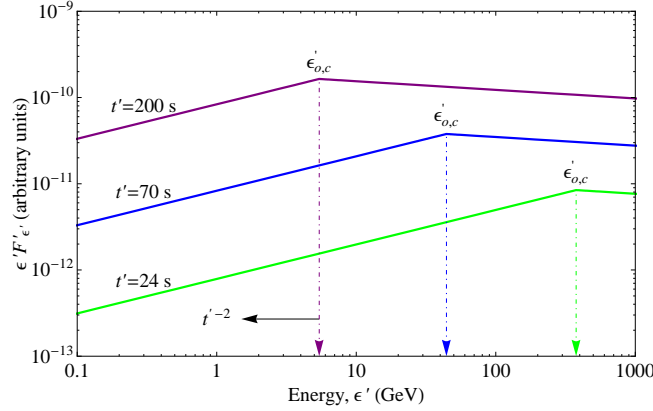


FIGURE 4. Proton synchrotron radiation spectrum at three different times $t' > \epsilon'_{o,c}$. Note that the peak of the synchrotron radiation spectrum $\epsilon'_{o,c}$ decreases with time as t'^{-2} as indicated by the arrows. The spectrum is $\propto \epsilon'^{-(\kappa-1)/2}$ below $\epsilon'_{o,c}$ and $\propto \epsilon'^{-\kappa/2}$ above $\epsilon'_{o,c}$, where $\kappa \gtrsim 2$ is the spectral index for shock-accelerated protons.

adopted here, in the 1 keV – 1 GeV range, typical of a bright long duration GRB — synchrotron radiation is the dominating energy loss channel for UHE protons for the model parameters $\epsilon_B/\epsilon_e \gtrsim 1$, the acceleration parameter $\phi \approx 1$ and for the variability time scale $t_v \gtrsim 10^{-3}$ s. An SSC component of high-energy γ -rays, which are expected to form simultaneously with keV–MeV synchrotron photons, is suppressed in the case $\epsilon_B/\epsilon_e \gtrsim 1$ as well. Photohadronic ($p\gamma$) interactions can dominate the energy losses by UHE protons if the GRB fireball is highly compact with ~ 1 ms scale variability or more target soft photons in the fireball than considered here, and for $\epsilon_B/\epsilon_e < 1$. In this case an SSC component is expected. We also found that proton synchrotron radiation and associated electromagnetic cascade emission, from synchrotron photons or/and pion-decay secondaries from $p\gamma$ interactions, can produce high-energy γ -rays which are delayed compared to the prompt keV–MeV emission. The delay is due to the time required for protons to be accelerated to UHE when they suffer large energy losses.

ACKNOWLEDGMENTS

Work supported by the Office of Naval Research and NASA grants.

REFERENCES

1. T. Piran, *Rev. Mod. Phys.*, **76**, 1143 (2005).
2. P. Mészáros, *Rep. Prog. Phys.*, **69**, 2259 (2006).
3. E. Waxman, *Phys. Rev. Lett.*, **75**, 386 (1995).
4. E. Waxman, and J. N. Bahcall, *Phys. Rev. Lett.*, **78**, 2292 (1997).
5. J. P. Rachen, and P. Mészáros, *Phys. Rev. D*, **58**, 123005 (1998).
6. C. D. Dermer, and A. Atoyan, *Phys. Rev. Lett.*, **91**, 071102 (2003).
7. S. Razzaque, P. Mészáros, and B. Zhang, *Astrophys. J.*, **613**, 1072 (2004).
8. K. Murase, and S. Nagataki, *Phys. Rev. D*, **73**, 063002 (2006).
9. K. Asano, and S. Inoue, *Astrophys. J.*, **671**, 645 (2007).
10. N. Gupta, and B. Zhang, *MNRAS*, **380**, 78 (2007).
11. S. Razzaque, O. Mena, and C. D. Dermer, *Astrophys. J. Lett.*, **691**, L37 (2009).
12. D. Band et al. *Astrophys. J.*, **413**, 281 (1993).
13. Y. Lithwick, and R. Sari, *Astrophys. J.*, **555**, 540 (2001).
14. C. D. Dermer, “Photoabsorption of Gamma Rays in Astrophysical Jets” in *The Tenth Marcel Grossmann Meeting*, edited by M. Novello et al., World Scientific, Singapore, 2005, pp. 1385.
15. C. D. Dermer, *Astrophys. J.*, **664**, 384 (2007).
16. R. Sari, and A. Esin, *Astrophys. J.*, **548**, 787 (2001).
17. R. Sari, T. Piran, and R. Narayan, *Astrophys. J. Lett.*, **497**, L17 (1998).